Electronic Supplementary Material (ESI) for Journal of Materials Chemistry C.

Supplementary Information

for

Comfortable skin sunscreens based on waterborne cross-linkable polydimethylsiloxane coatings

Ping Li[a], Shen Wang[b] and Shuxue Zhou[a,] *

a Department of Materials Science and State Key Laboratory of Molecular Engineering of Polymers, Advanced Coatings Research Center of Ministry of Education of China, Fudan University, Shanghai 200433, China.

b Shanghai Ninth People's Hospital, Shanghai Jiaotong University School of Medicine, Shanghai 200025, China.

* Corresponding author: Shuxue Zhou

E-mail address: zhoushuxue@fudan.edu.cn

1. Supplementary methods

1.1 Materials

Trichloromethane (≥99.0%), methanol (AR, ≥99.5%) and NaOH (AR, ≥96.0%) were obtained from Dahe Chemical Co., Ltd (Shanghai, China). $Al(NO_3)_3 \cdot 9H_2O$ (99.99% metals basis), $Mg(NO_3)_2 \cdot 6H_2O$ (AR, ≥99.0%), and $Fe(NO_3)_3 \cdot 9H_2O$ (98%) were purchased from Sinopharm Chemical ReagentCo., Ltd (Shanghai, China).

1.2 Synthesis of Mg/Al+Fe LDHs

Mg/Al+Fe LDHs were synthesized through a simple solvothermal process as follows. Briefly, $Al(NO_3)_3 \cdot 9H_2O$ and $Fe(NO_3)_3 \cdot 9H_2O$ with the Al^{3+}/Fe^{3+} molar ratio of 2.76/0.24 mmol, and 6.0 mmol of $Mg(NO_3)_2 \cdot 6H_2O$ were dissolved in 20 mL methanol, and then added dropwise into 80 mL NaOH-methanol solution (0.225 M). Afterward, the mixture was transferred to a 150 mL Teflon-lined autoclave and aged at 150°C for 18 h. The resulting suspension was centrifuged, and the precipitate was washed several times with deionized water until the pH value of the dispersion was close to 7. Without drying, the as-obtained wet precipitate was subsequently re-dispersed ultrasonically in deionized water to prepare transparent Mg/Al+Fe LDHs aqueous dispersion (Defined as I, concentration: 2 wt%) for further use.

Furthermore, the Mg/Al+Fe LDHs powder for characterization was obtained by placing the precipitate in a vacuum freeze dryer (Alpha 1-2 LDplus, Germany). The Mg/Al+Fe LDHs aqueous dispersion (concentration: 1 wt%) was then dropped onto a clean quartz glass slide (25 × 75 mm^2) and dried at ambient temperature to produce the transparent Mg/Al+Fe LDHs self-supporting inorganic film.

1.3 Characterization

Thermogravimetric analysis (TGA, Tecnai G20, A54, Netherlands) was carried out under a nitrogen atmosphere from 50°C to 800°C at a heating rate of 10 °C/min. The X-ray photoelectron spectroscopy (XPS, Perkin-Elmer PHI 5000C ECSA, USA) was performed using Al Kα radiation at a 90° take-off angle. XRD patterns were

recorded using an X'pert PRO X-ray diffractometer (PANalytical, Netherlands) with Cu Kα radiation. The morphology of Mg/Al+Fe LDHs was observed under transmission electron microscope (TEM, Tecnai G2 20 TWIN, A29, FEI Corp. USA) at an accelerating voltage of 200 kV. The size distribution and zeta potential of Mg/Al+Fe LDHs aqueous dispersion were measured by dynamic light scattering (DLS) method using a Zetasizer Nano-ZS90 instrument (Malvern, UK). The surface morphology of the dried film was inspected by a field emission scanning electron microscope (FESEM, Ultra 55, A28, Zeiss, Germany) at an accelerating voltage of 30 kV.

The surface tack of the dried sunscreen was determined by the blowing cotton ball method according to China National Standard GB/T 1728-1979 (1989) for paints and putties. Degreased cotton ball with about volume of 1 cm^3 was put on the surface of the sunscreen, and the cotton ball was gently blown along the horizontal direction with a mouth. If the cotton ball can be blown away without leaving the cotton silk, the surface is considered to be dry. Similarly, the dyed fumed silica powder was additionally adopted to verify the surface tack of the dried sunscreen.

2 Results and discussion

2.1 Synthesis and characterization of Mg/Al+Fe LDHs

Fig. S1a shows the TEM images of Mg/Al+Fe LDHs, which is well consistent with the result of size distribution measured by DLS (Fig. S1b). The as-obtained Mg/Al+Fe LDHs exhibited a nanosheet shape and were uniformly dispersed in deionized water with Z-average size of 82 nm. As shown in Fig. S1c, Mg/Al+Fe LDHs aqueous dispersion had a high surface zeta potential of +45 mV when freshly prepared, and +42 mV even after storage for three months. These facts well confirmed its excellent dispersibility and high storage stability. Two stages of the main mass loss were observed from the TGA curve of Mg/Al+Fe LDHs (Fig. S1d). They were

respectively the first stage below 260°C (weight loss: 11%) corresponding to the removal of physically absorbed and interlayer bound water molecules, and the second stage ranging from 260-550°C (weight loss: 38%) ascribed to the dehydroxylation of the LDH layers, indicating the good thermostability of Mg/Al+Fe LDHs. Additionally, the presence of Mg, Al, Fe, and O elements further confirmed the successful doping of Fe^{3+} into Mg/Al LDHs, which was verified by the XPS spectrum of Mg/Al+Fe LDHs (Fig. S1e). XPS analysis also shows the content of Mg, Al, and Fe were 14.3 mol%, 5.5 mol%, and 0.6 mol%, respectively, implying the high doping efficiency of Fe^{3+}. Fig. S1f demonstrates that Mg/Al+Fe LDHs aqueous dispersion (concentration: 0.1 wt%) can block the whole UV region (200-400 nm), but was highly transparent in the visible region, ensuring the feasibility of preparing the transparent UV-shielding coating. Besides, Mg/Al+Fe LDHs can form the inorganic films by themselves at ambient temperature. Fig. S1g further shows the UV-vis transmittance spectrum of Mg/Al+Fe LDHs self-supporting film (thickness: ~10 μm). It was obviously found that almost all UV lights below 400 nm were blocked while the film itself was still highly transparent. XRD patterns shown in Fig. S1h indicate the structure difference between Mg/Al+Fe LDHs and its self-supporting film. Line a shows sharp and symmetric reflections for the (003) and (006) planes at low 2θ values, and weaker and less symmetric reflections at higher angle for the Mg/Al+Fe LDHs powder. In contrast, Line b exhibits the disappearance of any in-plane reflections ($h,\ k \neq 0$) at high angles for the self-supporting film. The significant difference further confirms the well-oriented assembly of Mg/Al+Fe LDHs platelets within the film, ascribed to two types of interactions including close edge-to-edge and face-to-face packed perpendicular between individual platelets. It also can be seen from the typical surface FESEM images of the self-supporting film (Fig. S1i) with a rather smooth and flat surface. Overall, Mg/Al+Fe LDHs with the advantages of absorption bands over the whole UV region, excellent dispersibility in water, and outstanding UV-shielding performance, have been successfully synthesized that can be further adopted to act as a new inorganic UV shielding agent.

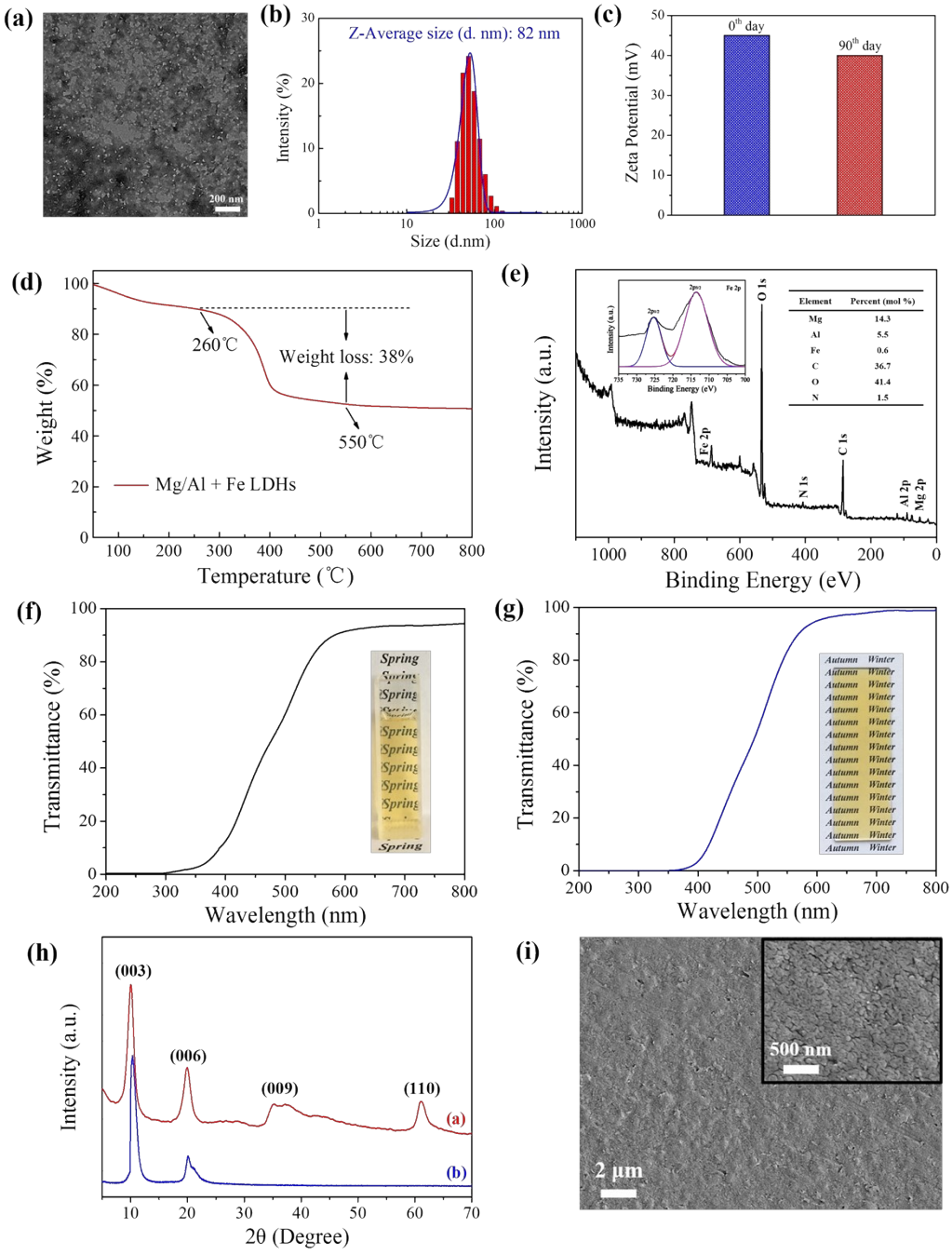

Fig. S1 (a) Typical TEM images, (b) size distribution measured by DLS, and (c) Zeta potential on 0th day and 90th day of Mg/Al+Fe LDHs aqueous dispersion. (d) TGA curve, and (e) XPS spectra of Mg/Al+Fe LDHs. (f) UV-vis transmittance spectrum and photograph (inset) of 0.1 wt% Mg/Al+Fe LDHs aqueous dispersion. (g) UV-vis transmittance spectrum and photograph (inset) of Mg/Al+Fe LDHs self-supporting film (thickness: ~10 μm) prepared from 1 wt% Mg/Al+Fe LDHs aqueous dispersion.

(h) XRD patterns of Mg/Al+Fe LDHs (Line a) and its self-supporting film (Line b). (i) Typical surface FESEM images of Mg/Al+Fe LDHs self-supporting film.

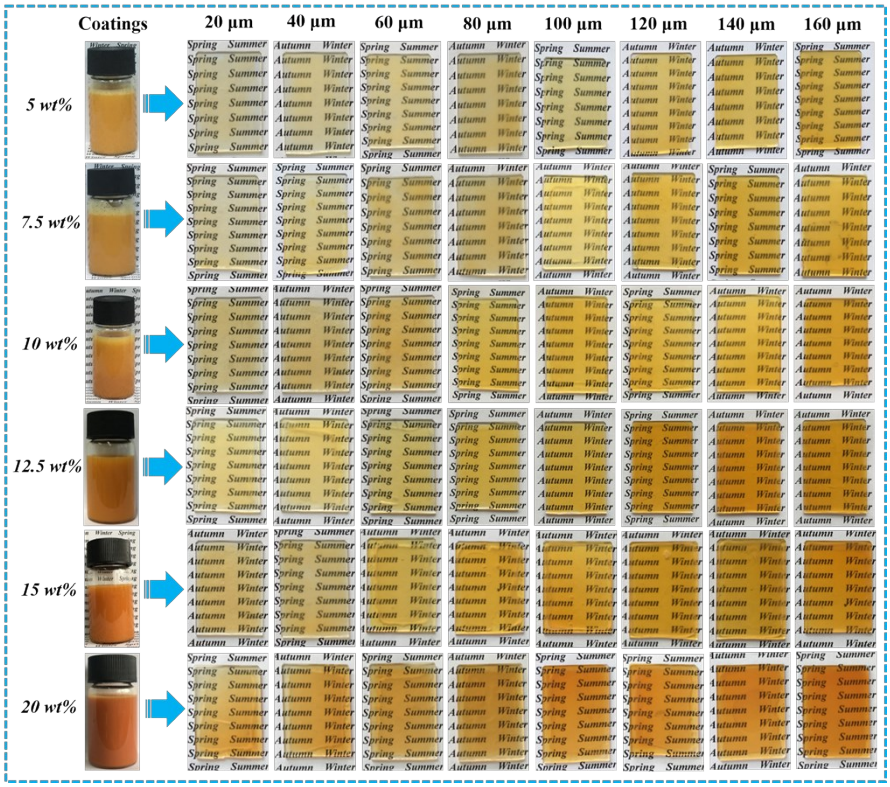

Fig. S2 Photographs of PI sunscreens with varied contents of Mg/Al+Fe LDHs and the corresponding PI coatings with different film thicknesses.

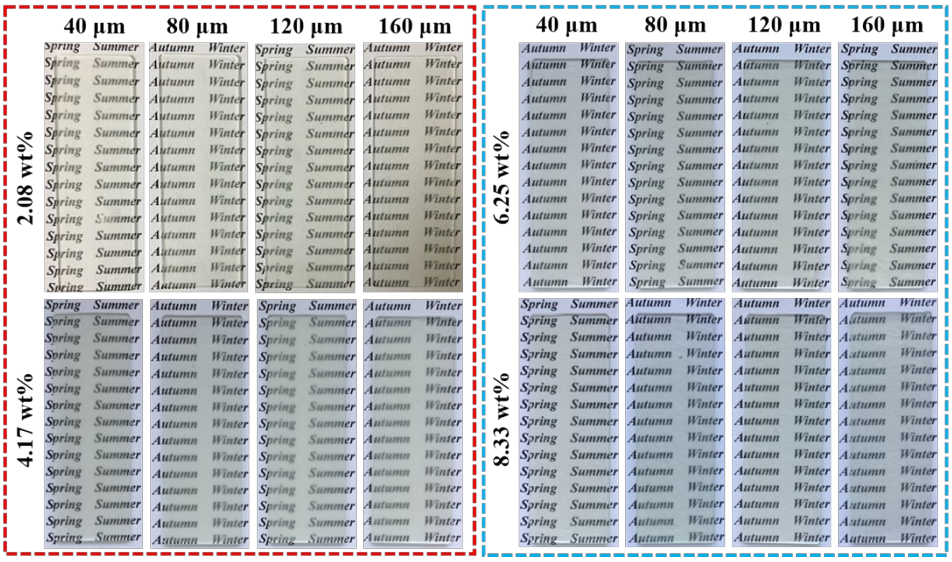

Fig. S3 Photographs of PO coatings with different film thicknesses at varied contents of organic UV absorber.

As intuitively presented in Fig. S4, both the degreased cotton ball and the dyed fumed silica powder were used to investigate the surface tack of the dried PO sunscreen. Clearly, the cotton ball was blown away without leaving the cotton silk, while the loose powder was left on the surface of PO sunscreen with 2.08~6.25 wt% of organic UV absorber. These surfaces were considered to be dry but still greasy. Furthermore, PO sunscreen with 8.33~11.65 wt% of organic UV absorber presented an increasingly sticky surface, that could be observed from the residual cotton silk or powder on its surface. The greasy or even sticky feeling of PO sunscreen was similar to the feeling of commercial sunscreens. In contrast, PI sunscreen showed an absolutely dry surface. Interestingly, addition of 0.69 wt% Mg/Al+Fe LDHs into the PO coating with 2.08 wt% organic UV absorber can efficiently eliminate its greasy surface, proving the advantage of POI sunscreen.

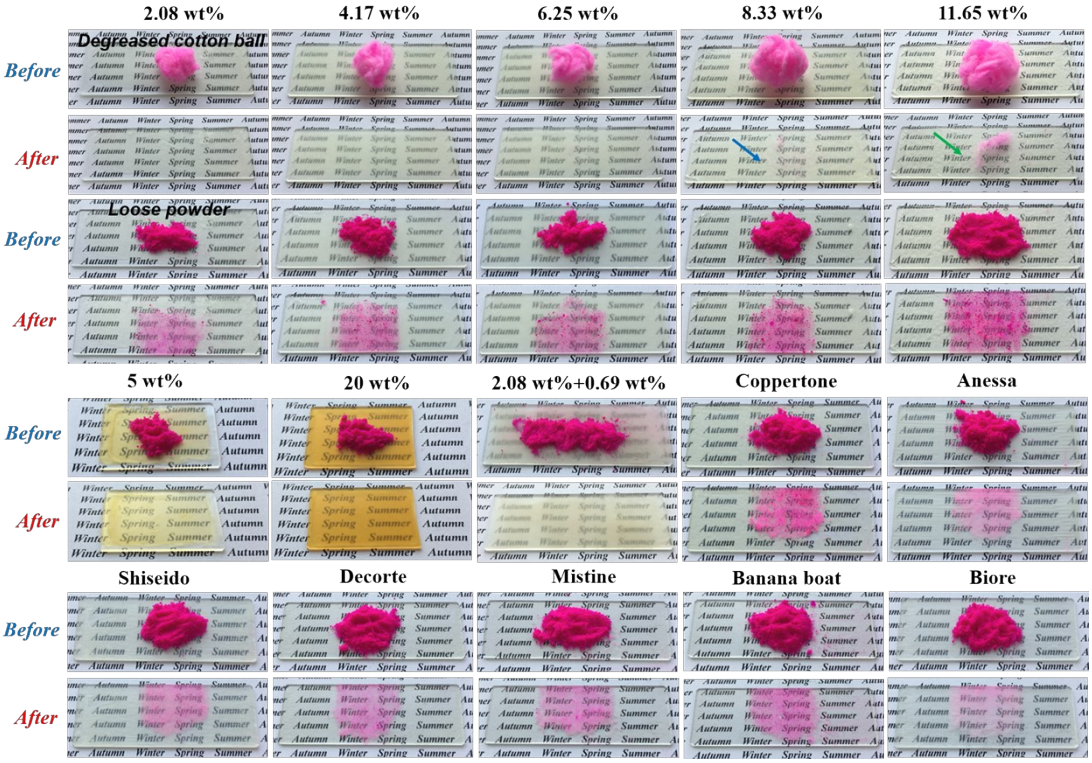

Fig. S4 The surface tack of PDMS-based sunscreens including PI sunscreen (5 wt%, 20 wt% Mg/Al+Fe LDHs), PO sunscreen (2.08~11.65 wt% organic UV absorber), POI sunscreen (2.08 wt% organic UV absorber + 0.69 wt% Mg/Al+Fe LDHs). Commercial sunscreens were used as the control. Before: put the degreased cotton ball or the dyed fumed silica powder on the surface of the dried sunscreen; After: blow away the degreased cotton ball or loose powder with a mouth.

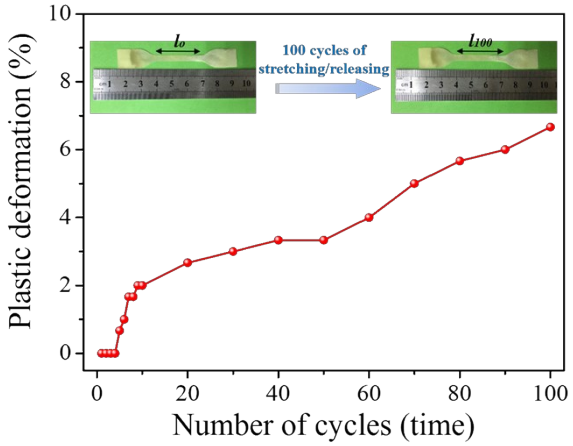

Fig. S5 The plastic deformation of PI coating with 10 wt% Mg/Al+Fe LDHs versus stretching/releasing cycles. Insets: photographs of PI coating (left) in initial state, and (right) in final state after 100 cycles of stretching/releasing.

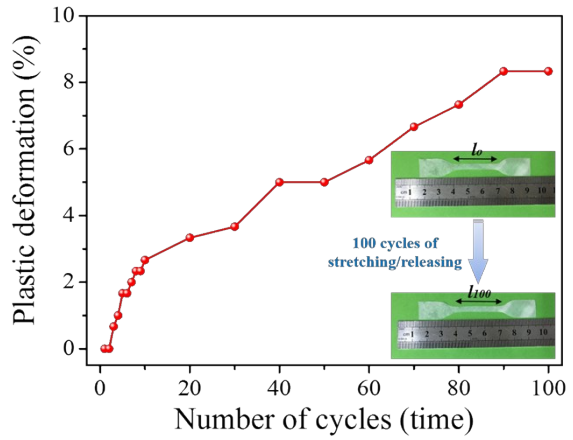

Fig. S6 The plastic deformation of PO coating with 2.08 wt% of organic UV absorber versus stretching/releasing cycles. Insets: photographs of PO coating (top) in initial state, and (bottom) in final state after 100 cycles of stretching/releasing.

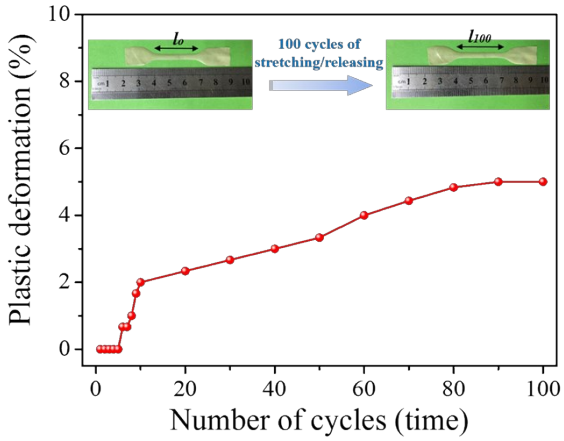

Fig. S7 The plastic deformation of POI coating with 2.08 wt% organic UV absorber and 0.69 wt% Mg/Al+Fe LDHs versus stretching/releasing cycles. Insets: photographs of POI coating (left) in initial state, and (right) in final state after 100 cycles of stretching/releasing.

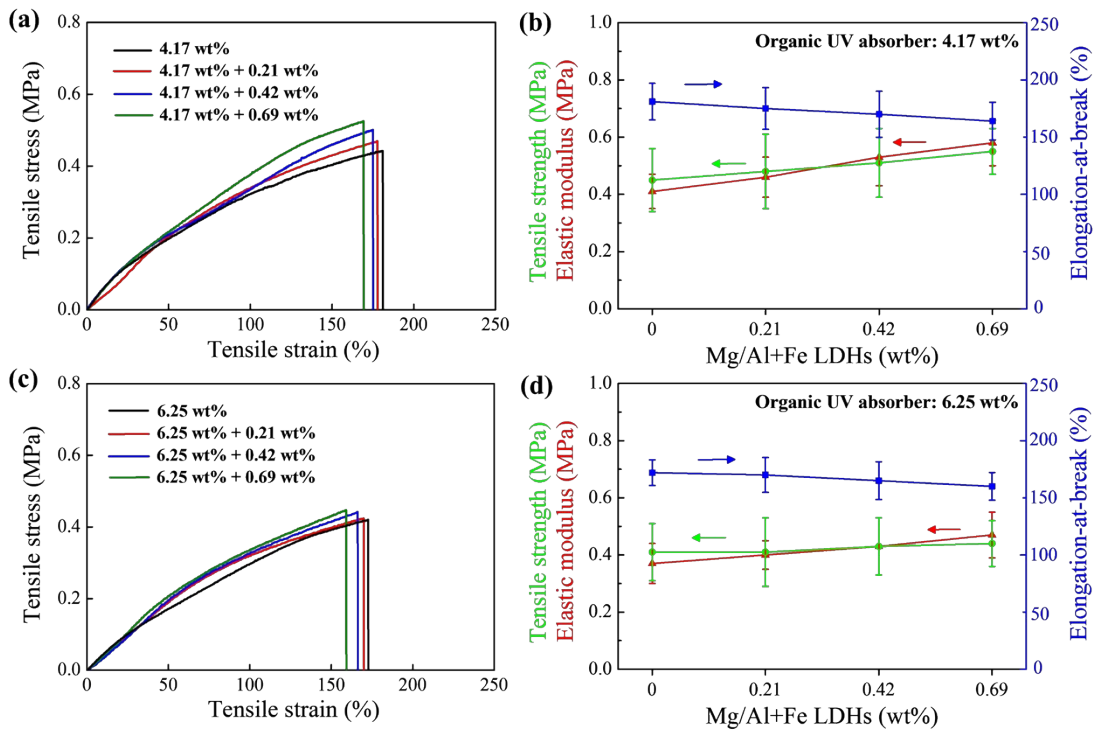

Fig. S8 (a, c) Stress-strain curves and (b, d) the mechanical properties (elastic modulus, tensile strength, and elongation-at-break) of POI coatings at (a, b) 4.17 wt%, and (c, d) 6.25 wt% organic UV absorber respectively, and varied contents of Mg/Al+Fe LDHs.

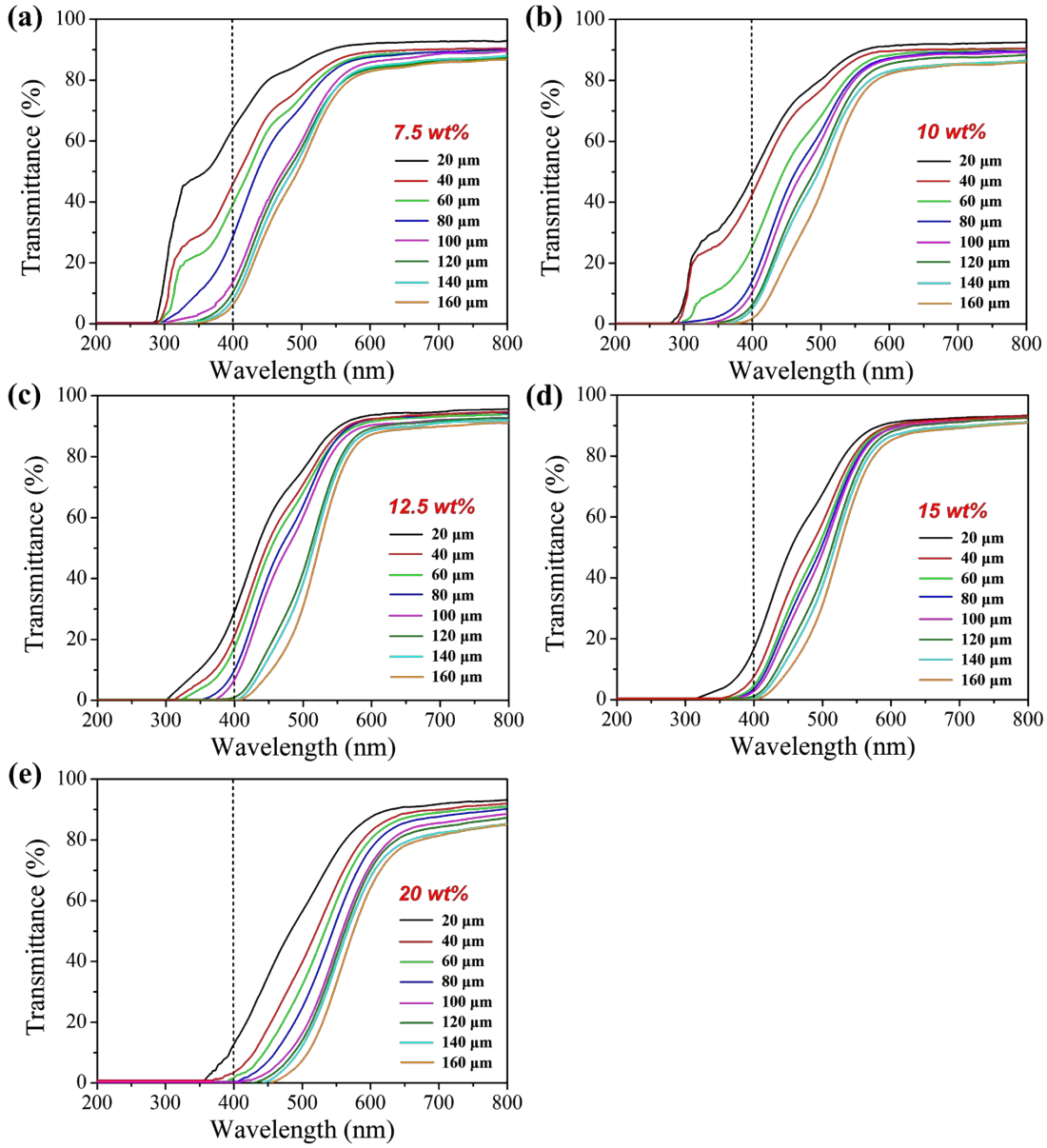

Fig. S9 UV-vis transmittance spectra of PI coatings with different film thicknesses at (a) 7.5 wt%, (b) 10 wt%, (c) 12.5 wt%, (d) 15 wt%, and (e) 20 wt% Mg/Al+Fe LDHs, respectively.

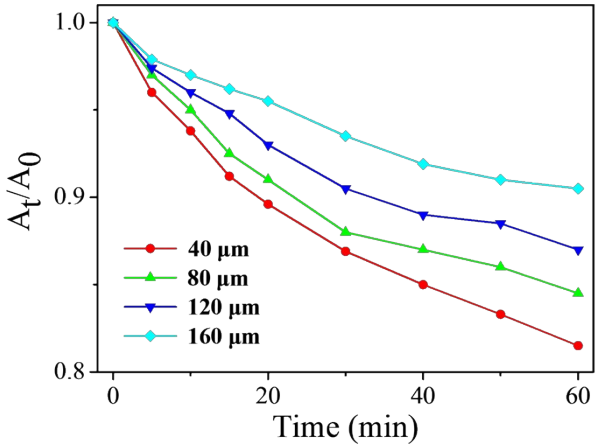

Fig. S10 Photodegradation curves for the Rhodamine B films protected by PO coatings with different film thicknesses at 2.08 wt% organic UV absorber (A_t and A_0 represent the absorbance at 552 nm at time t and the initial time, respectively).

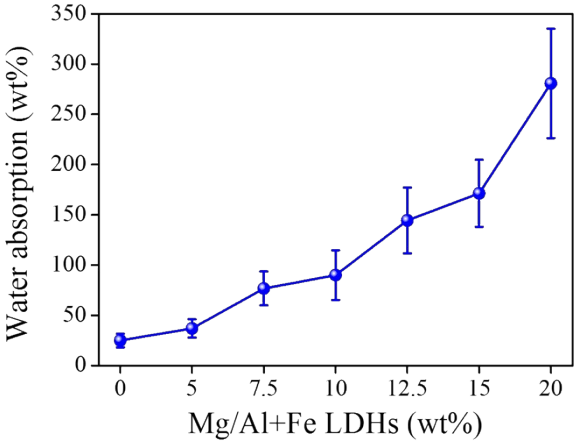

Fig. S11 Water absorption of PI coatings with varied contents of Mg/Al+Fe LDHs after submersion in deionized water.